PERGAMON

Journal of Structural Geology 24 (2002) 401–410

JOURNAL OF STRUCTURAL GEOLOGY

www.elsevier.com/locate/jstrugeo

Mechanical analysis of the geometry of forced-folds

Kaj M. Johnson*, Arvid M. Johnson

G.K. Gilbert Geomechanics Laboratory, Earth and Atmospheric Sciences, Purdue University, 1397 CIVL, West Lafayette, IN 47907, USA

Received 1 January 2001; accepted 1 August 2001

Abstract

A mechanical model of forced-folding, comprised of an anisotropic cover overlying displaced, rigid basement blocks, is used to investigate the influence of various parameters on theoretical fold form: shape and dip of basement fault, strength of basement-cover contact, and degree of anisotropy of the cover. We show that the degree of anisotropy in the cover largely influences the geometry of the forelimb of the forced-fold. Folds produced in isotropic cover display forelimbs that taper from large dip angles near the basement-cover contact to low dip angles at the ground surface. In contrast, dips in the forelimbs of folds in anisotropic cover are nearly uniform with depth. We show that the basement-cover contact and the shape of the basement fault largely influence the geometry of the backlimb. Backlimb rotation occurs in cover welded to the basement and in cover underlying curved basement faults. In addition, the kinematic features of the theoretical folds are compared with the fold geometry generated by parallel kink and trishear models. Folds in isotropic cover overlying straight basement faults closely resemble the fold forms produced by the trishear kinematic model while fold forms in anisotropic cover more closely resemble folds produced by parallel kink geometric constructions.

Keywords: Forced-folding; Isotropic; Anisotropic

1. Introduction

Typical structures in the Rocky Mountain Foreland of the western United States are fault-related folds that form over basement faults. Outcrops and seismic profiles show that the folds are typically asymmetric monoclines with long, gently-dipping backlimbs and short, steeply-dipping forelimbs, overlying straight or curved fault surfaces in basement rock (e.g. Prucha et al., 1965; Stearns, 1971; Reches, 1978; Stone, 1983a,b, 1985; Schmidt et al., 1993). Forced-folding has been proposed as the mechanism for some of these structures. The essential features of the forced-folding mechanism are a sedimentary cover that deforms more or less passively and rigid basement blocks that are displaced along planar or listic faults (Reches and Johnson, 1978; Stearns, 1978). Evidence for undeformed, perhaps rigid, basement blocks that moved during folding of the sedimentary cover has been cited in several folds in the Rocky Mountain Foreland (Prucha et al., 1965; Stearns, 1971; Mathews, 1986; Erslev et al., 1988; Erslev and Rogers, 1993).

Efforts to explain forced-folds have followed three, largely divergent paths: theoretical analysis, experimentation, and kinematic analysis. The earliest study was a combined experimental/theoretical analysis by Sanford (1959), who experimented with clay models and performed theoretical analyses with elasticity theory. Several researchers have theoretically analyzed the deformation of a single layer or multi-layer overlying a buried fault in an underlying, dissimilar material. Reches and Johnson (1978) and Haneberg (1992, 1993) examined the deformation of elastic layers overlying effectively rigid, displaced forcing blocks. Rodgers et al. (1981) analyzed the folding of an elastic layer overlying an elastic half-space containing an inclined edge dislocation. Patton and Fletcher (1995, 1998) developed a mechanical model using viscous folding theory, in which a linear or power-law layer overlies displaced, rigid blocks.

Numerous experimental studies of forced-folding have been carried out using clay and rock. For example, Withjack et al. (1990) performed clay experiments of forced-folds over normal faults and Friedman et al. (1980) formed small forced-folds experimentally in rock specimens subjected to high pressures.

Kinematic models and geometric constructions are methods commonly used in the structural geology literature to describe forced folds. The parallel kink construction of basement-involved folding by Narr and Suppe (1994) assumes that bed length and cross-sectional area are preserved and bed thickness and limb dips are uniform

* Corresponding author. Now at: Geophysics Department, Stanford University, Stanford, CA 94305, USA.

E-mail address: kaj@pangea.stanford.edu (K.M. Johnson).

0191-8141/02/$ - see front matter
PII: S0191-8141(01)00085-2

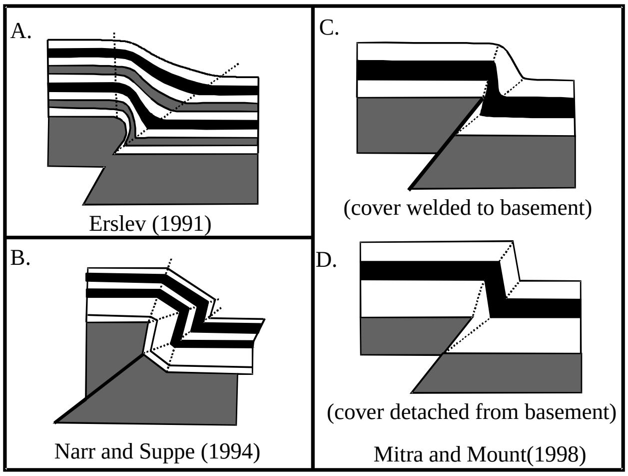

Fig. 1. Kinematic descriptions of forced-folds. Each model has a deformed cover overlying a rigid basement. The essential differences are in the deformation patterns assumed in the cover.

(Fig. 1B). The folds are formed over faults composed of linked, straight-line segments. Mitra and Mount (1998) imagined two end-member descriptions of basement-involved structures (Fig. 1C and D) depending on whether the cover rock is welded to or detached from the basement. They assumed intuitively that deformation should be concentrated within a triangular zone if the cover was welded to the basement and within a rectangular zone if the cover was detached from the basement. A third method, the trishear kinematic model, was introduced by Erslev (1991) and later expounded by Hardy and Ford (1997), Allmendinger (1998), and Zehnder and Allmendinger (2000). Trishear was invented to produce 'more nearly realistic' fold geometries with rounded hinges and variable forelimb dip angles (Fig. 1A). Trishear folds are formed by specifying a velocity distribution within the triangular region that satisfies the continuity equation (conservation of area).

In this paper we use a slight modification of the mechanical analysis of forced-folds presented by Patton and Fletcher (1995, 1998) to systematically investigate effects of various mechanical properties on fold form, and to compare the kinematic features, including fold geometry, produced by the theoretical analysis with those suggested by the various kinematic models. We will show that there are mechanical conditions under which parallel kink and trishear-like geometry could appear.

2. Mechanical model of basement forced-folding

Our model[1] of forced-folding uses the theory for plane flow of an incompressible, anisotropic viscous material. Our analyses of forced folding are based on the following specific assumptions:

1. The basement consists of two rigid blocks separated by a fault. One block translates relative to the other along a planar fault or rotates along a curved fault.
2. The velocity normal to the contact between the basement and the cover is conserved across the basement-cover contact.
3. The sedimentary cover is adequately modeled as a single anisotropic (isotropic) viscous layer. The anisotropy may be specified by the ratio, μ_n/μ_s, of the normal, μ_n, to the shear, μ_s, coefficients of viscosity (Fig. 2).
4. The sedimentary cover satisfies force equilibrium and conditions of incompressibility and continuity so that its behavior is described by a form of the biharmonic partial differential equation (see Patton and Fletcher (1995, 1998)).
5. The upper surface of the nonlinear material is the traction-free ground surface; that is, we specify that the tractions acting on the upper surface are zero.
6. The resistance to slip at the contact between the top of the basement and the bottom of the sedimentary cover can be modeled by placing a thin film at the cover-basement contact that controls the amount of shear passed from the basement to the cover. By varying the ratio, $\mu_f/\sqrt{\mu_n\mu_s}$, of the film viscosity, μ_f, to the effective cover viscosity, we can vary the resistance to slip at the contact ranging from free slip when $\mu_f/\sqrt{\mu_n\mu_s} = 0$ to welded when $\mu_f/\sqrt{\mu_n\mu_s} \gg 1$.

3. Influence of anisotropy on fold form

3.1. Anisotropy

The development of folds in basement-cored structures could be influenced by the mechanical anisotropy of the sedimentary cover (Spang and Evans, 1988) because mechanical anisotropy and properties of contacts between layers are known to largely control fold form in buckling of multilayers (e.g. Johnson, 1977; Johnson and Pfaff, 1989). We can express the anisotropy of multilayered rocks in terms of a viscosity ratio, μ_n/μ_s, for flowage of rocks (Fig. 2). The viscosity ratio is the ratio of the viscosity for shortening or lengthening parallel to layers, μ_n, to the viscosity for shearing parallel to layers μ_s. On this basis, there are three general categories of behavior. If the viscosity ratio is equal to one, the rock is *isotropic*. If the viscosity ratio is less than one ($\mu_s > \mu_n$), the rock is *anisotropic* and *layer-parallel soft* to deformation. If the viscosity ratio is greater than one ($\mu_s < \mu_n$), the rock is *anisotropic* and *layer-parallel stiff* to deformation.

Multilayers composed of many thin layers with low resistance to sliding between layers are characterized by layer-parallel stiff ($\mu_n/\mu_s > 1$) responses to deformation

[1] A trial version of the computer program *Forced-fold* may be downloaded from the Department of Earth and Atmospheric Sciences, Purdue University, *Faux Pli Software* website: http://www.eas.purdue.edu/fauxpli/.

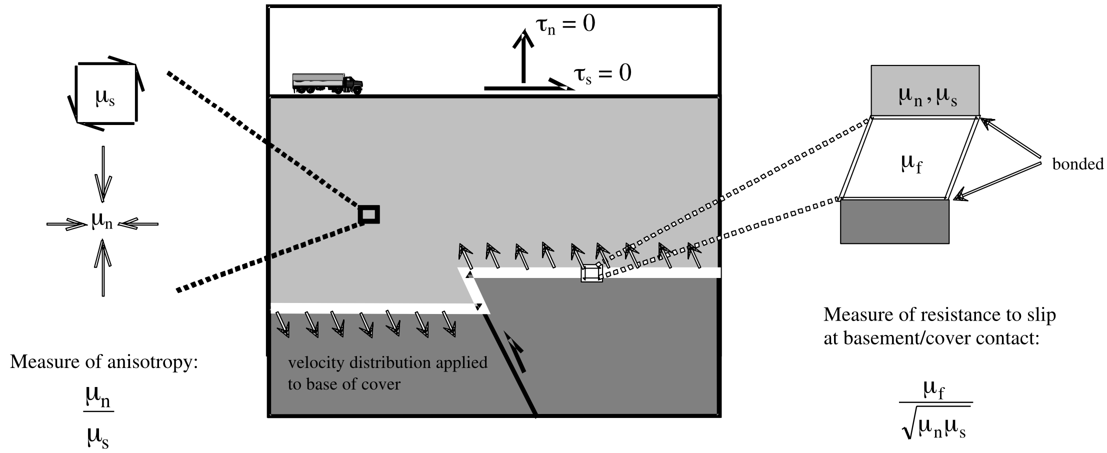

Fig. 2. Model parameters. Boundary conditions applied are a traction-free upper surface and a velocity distribution on the bottom interface. The anisotropy of the cover is specified by choosing a value for the ratio of the normal to shear velocity (μ_n/μ_s). A thin film is placed between the basement and the cover. The resistance to slip at the basement-cover contact is specified by choosing a ratio of the viscosity of the thin film, μ_f, to the effective viscosity $\mu_f/\sqrt{\mu_n \mu_s}$ of the cover.

(Biot, 1965; Johnson, 1977). In the same way, multilayers containing interbedded stiff and soft layers bonded together are layer-parallel stiff. Layer-parallel stiffness enhances flexural slip between stiff layers during folding and thus makes flexuring easy. In contrast, massively bedded, isotropic rock ($\mu_n/\mu_s = 1$) cannot deform by flexural slip and therefore makes bending more difficult. Bending is even more difficult if the layer is characterized as layer-parallel soft ($\mu_n/\mu_s < 1$). The layer tends to thicken or thin rather than to bend. Patton and Fletcher (1998) discuss conditions under which rock containing two sets of weak surfaces behaves as a layer-parallel soft material.

For layer-parallel stiff materials, the viscosity ratio has a clear physical interpretation. Consider the anisotropic medium as a multilayer consisting of bonded alternating stiff and soft isotropic layers with respective viscosities and thickness μ_1, t_1 and μ_2, t_2. The effective normal and shear viscosities of the multilayer can be expressed in terms of the layer viscosities and thickness:

$$\mu_s = \frac{t\mu_1\mu_2}{t_2\mu_1 + t_1\mu_2} \quad (1a)$$

$$\mu_n = \frac{t_1\mu_1 + t_2\mu_2}{t} \quad (1b)$$

where $t = t_1 + t_2$ (see Johnson (1977) pp. 48, 50 for a derivation). Thus the viscosity ratio is:

$$\frac{\mu_n}{\mu_s} = \frac{(t_1\mu_1 + t_2\mu_2)(t_1\mu_2 + t_2\mu_1)}{t^2\mu_1\mu_2} \quad (2)$$

We can immediately see that as the viscosity of the soft layer (μ_2) approaches zero, the viscosity ratio approaches infinity. That is to say, a large viscosity ratio models a multilayer with little resistance to slip between layers. If we let $t_1 = t_2$, Eq. (2) simplifies to:

$$\frac{\mu_n}{\mu_s} = \frac{\left(\frac{\mu_1 + \mu_2}{2}\right)^2}{\mu_1\mu_2} \quad (3)$$

Thus for layers of equal thickness with layer 1 ten times stiffer than layer 2, the viscosity ratio is about three.

Fig. 3 shows some examples of forced-folds produced with our mechanical model for basement faults of different types and for isotropic ($\mu_n/\mu_s \approx 1$) and anisotropic ($\mu_n/\mu_s = 3$) sedimentary covers. In all these examples the sedimentary cover was welded to the basement rocks ($\mu_f/\sqrt{\mu_n\mu_s} \gg 1$).

3.2. General results

The theoretical results show that the forelimb geometry is largely influenced by the anisotropy of the cover. In the isotropic cover, the forelimb tapers in width and dip from steep dip angles and narrow limbs near the fault tip to more shallow dip angles and wider limbs at the ground surface. In contrast, there is less tapering of forelimb width and dips in the anisotropic cover (Fig. 3). The walls of the forelimb are drawn with dashed lines in Fig. 3. The forelimb walls in the anisotropic cover are nearly parallel.

Fig. 4 displays fold forms and strain ellipses for covers with viscosity ratios ranging from $\mu_n/\mu_s = 1/3$ to 3. The right column of Fig. 4 plots the percent change in layer thickness (positive values correspond to thickening and negative values to thinning). It is evident from the contour plots that the deformation in the layer-parallel stiff cover is more highly localized within the forelimb than in the other two folds. The folds in the isotropic and layer-parallel soft covers (Fig. 4A and C) display greater thickening in the synclinal hinge than the fold in the layer-parallel stiff cover (Fig. 4B). The fold in the layer-parallel stiff cover

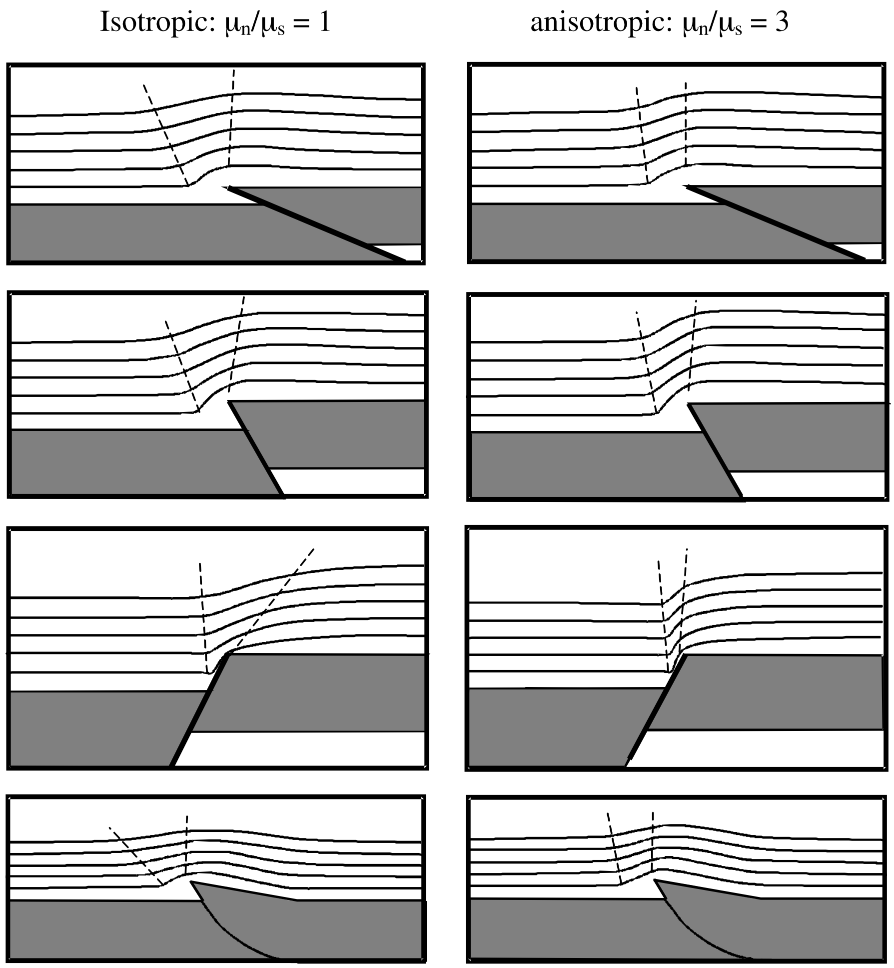

Fig. 3. Forced-folds produced with the mechanical model. Cover welded to the basement in each example. The loading in the model is provided entirely by the displaced rigid basement blocks. The fold shape is influenced by the geometry of the fault and the anisotropy of the cover. Dashed lines show the boundaries of the forelimb.

displays greater thinning through the forelimb than the other two folds.

3.3. Comparison with experiments

We will investigate the role of anisotropy on forms of forced-folds using the geometry of experimental examples. Friedman et al. (1980) conducted experiments using lubricated layers of limestone and sandstone. Lubricated rock layers were stacked over rigid forcing blocks with a 66° dipping fault and subjected to confining pressure. Lubrication of the rock layers was intended to create an anisotropic cover medium and encourage flexural slip during folding. Fig. 5A shows the deformed rock layers in Friedman et al.'s (1980) experiment.

We modeled the conditions of this experiment with our theory using an isotropic cover (Fig. 5B) and an anisotropic cover (Fig. 5C). The model with an anisotropic cover (viscosity ratio of $\mu_n/\mu_s = 2$) (Fig. 5F) provides a better fit to the experimental fold than the model with an isotropic ($\mu_n/\mu_s = 1$) cover, so the theoretical folds show that, indeed, the rock cover in the experiment behaved much like an anisotropic material.

As a counterproof, we compare our results with an experiment in which the cover should be isotropic. A forced-fold in clay material overlying a basement normal fault in an experiment by Withjack et al. (1990) is shown in Fig. 5D. We would expect a homogeneous block of clay to behave as an isotropic material. We modeled this normal fault using an isotropic cover (Fig. 5E) and an anisotropic cover (Fig. 5F). The results for the isotropic cover nearly perfectly fit the slopes and amplitudes of the top three layers of the clay model. In contrast, the slopes of the upper three layers in the anisotropic cover ($\mu_n/\mu_s = 2$) are too steep to fit the clay layers.

3.4. Comparison with trishear and parallel kink descriptions

The effect of anisotropy on fold form is shown in more detail in Fig. 6. The fold in the isotropic cover (Fig. 6A) broadens and shallows up section, whereas the fold in the

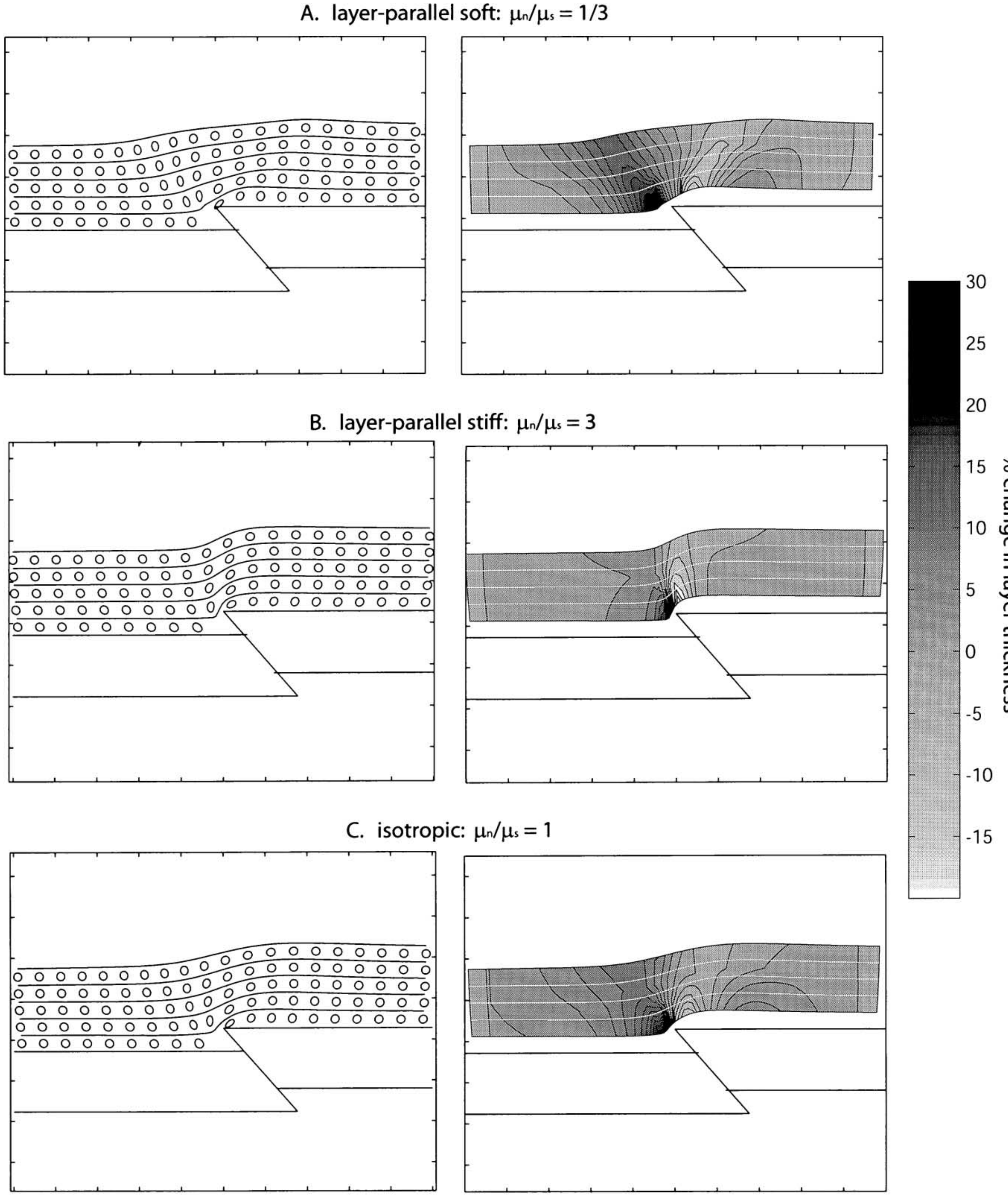

Fig. 4. Folds formed in isotropic and anisotropic covers overlying a 45° dipping reverse fault. In each example the cover is welded to the basement. Contour plots show the percent change in the thickness of the layers. The folds in the isotropic and layer-parallel soft cover display more thickening in the synclinal hinge than the fold in the layer-parallel stiff cover. The forelimb in the layer-parallel stiff cover displays more thinning than the forelimbs in the other two folds.

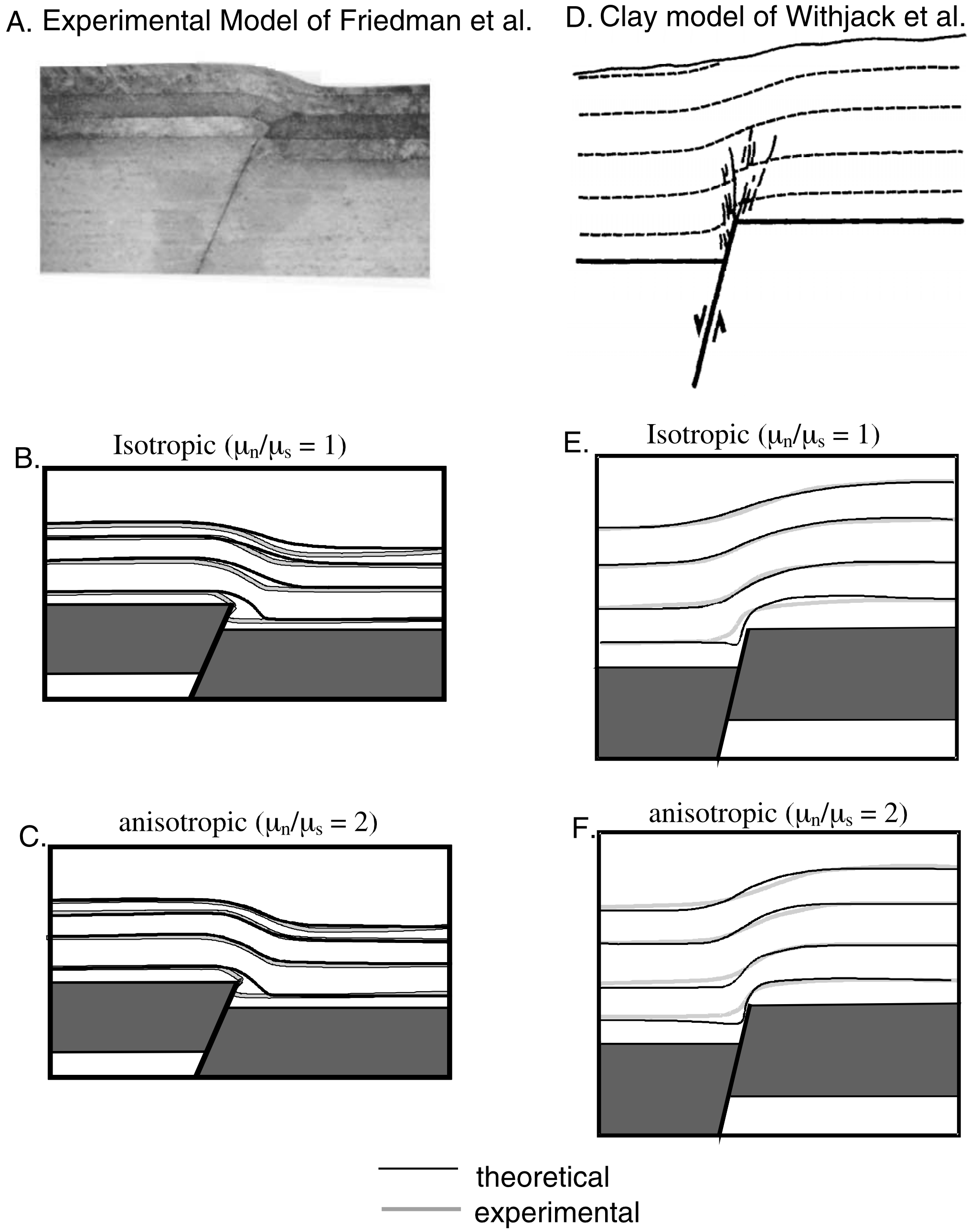

Fig. 5. Comparison of theory with experiments with lubricated rock (A–C), and clay (D–F). The lubricated rock layers are better modeled with an anisotropic ($\mu_n/\mu_s = 2$) cover, whereas the clay is better modeled as an isotropic cover.

highly anisotropic cover (Fig. 6C) has a nearly constant width and dip angle up section.

The geometry of the theoretical model with isotropic cover closely resembles the geometry produced by the trishear description and Mitra and Mount's welded cover model. The theoretical forelimb in Fig. 6A forms a triangular wedge with tapering forelimb width and dips, much like the forelimbs in Fig. 1A and C.

The forelimbs in the layer-parallel stiff, anisotropic covers in Fig. 6B and C have quite different geometries. The forelimb widths are nearly uniform with depth much like the idealized parallel kink folds of Narr and Suppe (1994) (Fig. 1B) and the idealized 'cover-detached folds' of Mitra and Mount (1998) (Fig. 1D). There is less variation in forelimb dips with depth in the anisotropic covers. The dips are essentially uniform in the highly anisotropic cover (Fig. 6C).

Although Mitra and Mount (1998) associated uniformly dipping forelimbs with cover detached from basement and tapering forelimbs with cover welded to basement, our modeling results suggest that the degree of anisotropy largely controls the forelimb geometry. We show in the next section that the nature of the basement/cover contact has less influence on forelimb geometry.

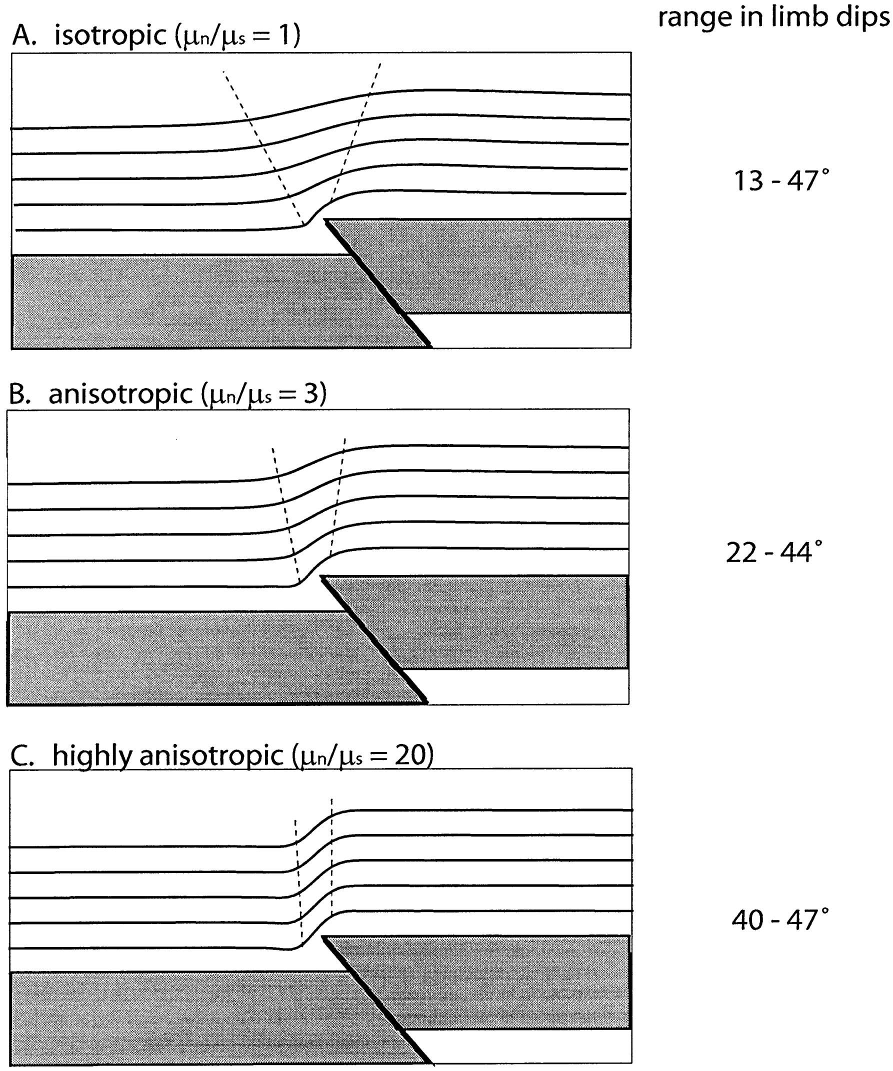

Fig. 6. Comparison of folds formed in isotropic and anisotropic covers above a 45° reverse fault in a rigid basement. Dashed lines are axial planes (boundaries of forelimb). Cover welded to basement.

4. Influence of basement-cover contact and shape of basement fault on fold form

Stearns (1978) documented that some folds in the Rocky Mountain Foreland are characterized by sedimentary bedding that is thinned in the steep forelimb (e.g. Uncompahgre uplift), while in others the bedding maintains nearly constant thickness above the basement-cover contact (e.g. Rattlesnake Mountain). Stearns deduced that whether the cover rock is thinned depends on the basement-cover contact — sedimentary cover that is nearly constant in thickness through the forelimb was detached from the basement, while cover rock that is thinned in the forelimb was welded to the basement. Others, though, apparently dispute Stearn's deduction. Hodgson (1965) and Blackstone (1981) point out that there is no evidence to suggest that detachments occur at the cover-basement contacts in the Rocky Mountain Foreland.

Mitra and Mount (1998) carried Stearn's deduction further, generalizing it by proposing two end-member models of forced folding depending on whether the cover units are welded to (Fig. 1C) or decoupled from (Fig. 1D) the basement. They supposed that, if the cover is welded to the basement, the forelimb has shallower dips distant from the basement fault and steeper dips near the basement fault. If the cover is detached from the basement, they suggest the forelimb dip angle is constant and the fold form resembles the parallel kink style of folding proposed by Narr and Suppe (1994).

With the mechanical model we can predict the influence of the basement-cover contact on the form of a forced-fold. We have added a thin film at the basement-cover contact into the mechanical model so we can vary the resistance to slip at the base of the cover (see Appendix A). We do so by varying the ratio of the viscosity of the film to a measure of the viscosity of the anisotropic cover through a parameter, $\mu_f/\sqrt{\mu_n\mu_s}$ (Fig. 2). A large ratio of $\mu_f/\sqrt{\mu_n\mu_s}$ simulates a cover welded to the basement (Fig. 7A). A small ratio of

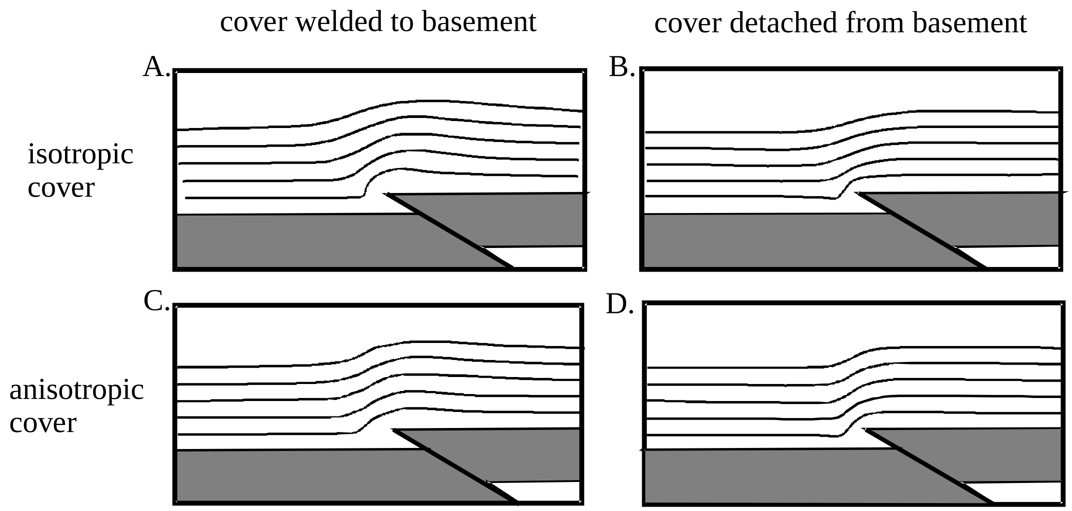

Fig. 7. Folds formed over a 30° dipping thrust fault. The folds in the welded cover display bulging of the anticlinal hinge and slight backlimb rotation. The folds in the detached cover display no backlimb rotation.

$\mu_f/\sqrt{\mu_n\mu_s}$ simulates a cover that is free to slip relative to the basement (Fig. 7B).

Fig. 7 shows four examples of solutions for low-angle, reverse faulting of a rigid basement overlain by homogeneous sedimentary cover; Fig. 7A and B shows homogeneous overburden and Fig. 7C and D shows anisotropic overburden. The figure demonstrates that the resistance to slip at the contact between the cover and basement has the largest influence on the anticlinal hinge and backlimb geometry. The anticlinal hinge in the welded cover (Fig. 7A) is amplified, bulged upward, more than in the detached cover (Fig. 7B). This apparently is a result of layer-parallel shortening induced in the cover by the reverse faulting in the basement. The fold in the welded cover displays a slight backlimb rotation that is not displayed in the fold in detached cover.

Based on this analysis, there appears to be no sound, mechanical reason to expect the deformation of the forelimb to reflect the nature of the basement-cover contact. Indeed, the theory shows that the change in forelimb shape is a result of the rheologic properties of the overburden, and the experiments by Friedman et al. (1980) and Withjack et al. (1990) support this conclusion. Clearly, the kink-like forms (Fig. 7C and D) occur in the anisotropic cover and widening-outward forms (Fig. 7A and B) occur in the isotropic cover, whether the cover is welded to or detached from the basement.

Backlimb rotation is a common feature of Rocky Mountain Foreland uplifts (e.g. Stone, 1993) and thus deserve some attention. Our theoretical models in Fig. 7 show a slight backlimb rotation of up to 10° in isotropic and anisotropic cover welded to the basement. However, basement-involved folds in, for example, the Big Horn Basin, Wyoming, exhibit much larger backlimb rotations of 20–30°. Larger backlimb rotation, comparable with that observed in the Big Horn Basin, is produced in the forced-fold model with a curved basement fault (Fig. 3).

5. Discussion and conclusions

Our model of forced-folds allows us to investigate the influence of (1) shape and dip of basement fault, (2) strength of basement-cover contact, and (3) degree of cover anisotropy on fold form. Figs. 3, 6 and 7 show that the geometry of the forelimb is largely influenced by the rheology of the cover and less influenced by the shape and dip of the basement fault and by resistance to slip at the basement-cover contact. In each of the folds produced in isotropic cover (left column of Fig. 3), the forelimb is thickened near the synclinal hinge and thinned between the anticlinal and synclinal hinges, regardless of the geometry of the basement fault. The degree of anisotropy in the cover, however, largely influences the geometry of the forelimb. In each of the folds produced in isotropic cover, the forelimb tapers from large dip angles near the basement-cover contact to low dip angles at the ground surface. In contrast, the dips of layering in the forelimb of folds in anisotropic cover are nearly uniform with depth (Fig. 6). The forelimbs in isotropic cover closely resemble the fold forms produced by the trishear kinematic description (Fig. 1A), while the forelimbs in the anisotropic cover more closely resemble the fold forms produced by the parallel kink construction of Narr and Suppe (1994) and Mitra and Mount (1998) (Fig. 1B–D). The theory of this study indicates conditions under which fold forms resembling the two quite different kinematic descriptions can be produced. The theory also indicates for all gradations of form between the end members.

We have also shown that the lubricated sandstone and limestone layers in the Friedman et al. (1980) experimental model behave much like a viscous material with anisotropy $\mu_n/\mu_s = 2$. The clay material in the Withjack et al. (1990) model has no slip surfaces and is best modeled with the anisotropic mechanical model.

We should emphasize here that this mechanical model is intended to help us understand the mechanism of forced-folding, and we do not suggest that this mechanism is appropriate for all basement-involved foreland structures. While some authors have suggested that some foreland folds formed over rigid, displaced basement blocks (Prucha et al., 1965; Stearns, 1971; Mathews, 1986; Erslev et al., 1988; Erslev and Rogers, 1993), others provide evidence that the basement is folded (Berg, 1962; Blackstone, 1983; Brown, 1984; Narr, 1993; Narr and Suppe, 1994). Basement-involved structures that involve folded basement may not form under the same mechanism as forced-folds. Similarly, the forced-fold theoretical model does not include propagation of faults from the basement into the cover.

Acknowledgements

We thank M. Cooke and B. Kilsdonk for reviewing the manuscript and M. Durdella for finding bugs in the forced-fold program. This work was performed under a Department of Energy grant (De-FG02-98ER14886), supervised by Nick Woodward of the DoE.

Appendix A. Treatment of basement-cover contact

We place a thin film between the basement and cover to allow the flexibility for variable resistance to slip at the basement-cover contact. A general method for a nonlinear, power-law viscous film is oulined in Johnson and Fletcher (1994). Here we use the case of a linear viscous film. The film is assumed to be so thin that it can deform only in simple shear. For plain strain, the shear stress parallel to the film is:

$$\sigma_{ns} = 2BD_{ns} \tag{A1}$$

where B is a material constant and D is deformation rate. The rate of shearing deformation is given by the rate of slip, δv_s, across the film:

$$D_{ns} \approx (1/2)(\delta v_s/h_f) \tag{A2}$$

where

$$\delta v_s = (v_s)_t - (v_s)_b \tag{A3}$$

h_f is the thickness of the film, and $(v_s)_t$ and $(v_s)_b$ are the velocities parallel to the film at the top and bottom surfaces, respectively. Thus at the bottom of the cover we have the boundary condition:

$$\delta v_s = (h_f/\mu_f)\sigma_{ns} \tag{A4}$$

References

Allmendinger, R.W., 1998. Inverse and forward numerical modeling of trishear fault-propagation folds. Tectonics 17 (4), 640–656.

Berg, R.R., 1962. Mountain flank thrusting in Rocky Mountain foreland, Wyoming and Colorado. American Association of Petroleum Geologists Bulletin 46, 219–232.

Biot, M.A., 1965. Mechanics of Incremental Deformations. John Wiley and Sons, New York.

Blackstone Jr, D.L., 1981. Compression as an agent in deformation of the east-central flank of the Bighorn Mountains, Sheridan and Johnson Counties, Wyoming. University of Wyoming Contributions to Geology 22, 1–38.

Blackstone Jr, D.L., 1983. Laramide compressional tectonics, southeastern Wyoming. University of Wyoming Contributions to Geology 19, 105–122.

Brown, W.G., 1984. Basement involved tectonics — foreland areas. American Association of Petroleum Geologists Continuing Education Course Note Series, no. 26, 92pp.

Erslev, E.A., 1991. Trishear fault-propagation folding. Geology 19, 617–620.

Erslev, E.A., Rogers, J.L., 1993. Basement-cover geometry of Laramide fault-propagation folds. In: Schmidt, C.J., Chase, R.B., Erslev, E.A. (Eds.). Laramide Basement Deformation in the Rocky Mountain Foreland of the Western United States. Geological Society of America Special Paper 280, pp. 125–146.

Erslev, E.A., Rogers, J.L., Harvey, M., 1988. The northeastern Front Range revisited: horizontal compression and crustal wedging in a classic locality for vertical tectonics. In: Holden, G.S. (Ed.). Geological Society of America Field Trip Guide. Colorado School of Mines Professional Contributions, 12, pp. 122–133.

Friedman, M., Hugman III, R.H.H., Handin, J., 1980. Experimental folding of rocks under confining pressure, part VIII — forced folding of unconsolidated sand and lubricated layers of limestone and sandstone. The Geological Society of America Bulletin 91, 307–312.

Haneberg, W.C., 1992. Drape folding of compressible elastic layers: I. Analytical solutions for vertical uplifts. Journal of Structural Geology 14 (6), 713.

Haneberg, W.C., 1993. Drape folding of compressible elastic layers: II. Matrix solution for two-layer folds. Journal of Structural Geology 15 (7), 923–932.

Hardy, S., Ford, M., 1997. Numerical modeling of trishear fault propagation folding. Tectonics 16 (5), 841–854.

Hodgson, R.A., 1965. Genetic and geometric relations between structures in basement and overlying sedimentary rocks with examples from Colorado Plateau and Wyoming. American Association of Petroleum Geologists 49, 935–949.

Johnson, A.M., 1977. Styles of Folding. Elsevier, New York.

Johnson, A.M., Pfaff, V.J., 1989. Parallel, similar and constrained folds. Engineering Geology 27, 115–180.

Johnson, A.M., Fletcher, R.F., 1994. Folding of Viscous Layers. Columbia University Press, New York.

Mathews III, V., 1986. A case for brittle deformation of the basement during the Laramide Revolution in the Rocky Mountain foreland province. Mountain Geologist 23, 1–5.

Mitra, S., Mount, V.S., 1998. Foreland basement-involved structures. American Association of Petroleum Geologists 82 (1), 70–109.

Narr, W., 1993. Deformation of basement in basement-involved, compressive structures. In: Schmidt, C.J., Chase, R.B., Erslev, E.A. (Eds.). Laramide Basement Deformation in the Rocky Mountain Foreland of the Western United States. Geological Society of America Special Paper, 280, pp. 107–124.

Narr, W., Suppe, J., 1994. Kinematics of basement-involved compressive structures. American Journal of Science 294, 802–860.

Patton, T.L., Fletcher, R.C., 1995. Mathematical block-motion model for deformation of a layer above a buried fault of arbitrary dip and sense of slip. Journal of Structural Geology 17 (10), 1455–1472.

Patton, T.L., Fletcher, R.C., 1998. A rheological model for fractured rock. Journal of Structural Geology 20 (5), 491–502.

Prucha, J.J., Graham, J.A., Nickelson, R.P., 1965. Basement controlled deformation in Wyoming provinces of Rocky Mountain foreland. American Association of Petroleum Geologists Bulletin 49, 966–992.

Reches, Z., 1978. Structure of the Palisades Creek branch of the East Kaibab monocline, Grand Canyon, Arizona. In: Mathews III, V. (Ed.). Laramide Folding Associated with Basement Block Faulting in the Western United States. Geological Society of America Memoir, 151, pp. 235–271.

Reches, Z., Johnson, A.M., 1978. Theoretical analysis of monoclines. In: Mathews III, V. (Ed.). Laramide Folding Associated with Basement Block Faulting in the Western United States. Geological Society of America Memoir, 151, pp. 273–311.

Rodgers, D.A., Gallagher Jr, J.J., Rizer, W.D., Spang, J.H., 1981. Deformation and secondary faulting near the leading edge of a thrust fault. Geological Society Special Publication 9, 65.

Sanford, A.R., 1959. Analytical and experimental study of simple geologic structures. Geological Society of America Bulletin 70, 19–52.

Schmidt, C.J., Chase, R.B., Erslev, E.A. (Eds.), 1993. Laramide Basement Deformation in the Rocky Mountain Foreland of the Western United States. Geological Society of America Special Paper, 280.

Spang, J.H., Evans, J.P., 1988. Geometrical and mechanical constraints on basement-involved thrusts in the Rocky Mountain foreland province. Geological Society of America Memoir 171, 41–51.

Stearns, D.W., 1971. Mechanisms of drape folding in the Wyoming Province. In: Renfro, A.R. (Ed.). Symposium on Wyoming Tectonics and their Economic Significance. pp. 125–143 Wyoming Geological Association, Annual Field Conference 23rd Guidebook.

Stearns, D.W., 1978. Faulting and forced folding in the Rocky Mountain foreland. Geological Society of America Memoir 151, 1–38.

Stone, D.S., 1983a. Seismic profile: South Elk Basin area, Big Horn Basin. In: Bally, A.W. (Ed.). Seismic Expression of Structural Styles. American Association of Petroleum Geologists, 3.2.2, pp. 20–24.

Stone, D.S., 1983b. Seismic profile: North Fork area, Powder River Basin, Wyoming. In: Bally, A.W. (Ed.). Seismic Expression of Structural Styles. American Association of Petroleum Geologists, 3.2.2, pp. 15–19.

Stone, D.S., 1985. Geologic interpretation of seismic profiles, Big Horn Basin, Wyoming. Part I: East Flank. In: Gries, R.G., Dyer, R.C. (Eds.). Seismic Exploration of the Rocky Mountain Region. Rocky Mountain Association of Geologists and Denver Geophysical Society, Folio, 1, pp. 165–174.

Stone, D.S., 1993. Basement-involved thrust-generated folds as seismically imaged in the subsurface of the central Rocky Mountain foreland. In: Schmidt, C.J., Chase, R.B., Erslev, E.A. (Eds.). Laramide Basement Deformation in the Rocky Mountain Foreland of the Western United States. Geological Society of America Special Paper, 280, pp. 271–318.

Withjack, M.O., Olson, J., Peterson, E., 1990. Experimental models of extensional forced folds. The American Association of Petroleum Geologists Bulletin 74 (7), 1038–1054.

Zehnder, A.T., Allmendinger, R.W., 2000. Velocity field for the trishear model. Journal of Structural Geology 22, 1009–1014.